

Available online at www.sciencedirect.com

ScienceDirect

www.elsevier.com/locate/jes

Variability of PM_{2.5} and O₃ concentrations and their driving forces over Chinese megacities during 2018–2020

Tianyi Xu^{1,4}, Chengxin Zhang^{2,*}, Cheng Liu^{2,3,4,5,*}, Qihou Hu⁴

¹School of Environmental Science and Optoelectronic Technology, University of Science and Technology of China, Hefei 230026, China

²Department of Precision Machinery and Precision Instrumentation, University of Science and Technology of China, Hefei 230026, China

³Center for Excellence in Regional Atmospheric Environment, Institute of Urban Environment, Chinese Academy of Sciences, Xiamen 361021, China

⁴Key Laboratory of Environmental Optics and Technology, Anhui Institute of Optics and Fine Mechanics, Chinese Academy of Sciences, Hefei 230031, China

⁵Key Laboratory of Precision Scientific Instrumentation of Anhui Higher Education Institutes, University of Science and Technology of China, Hefei 230026, China

ARTICLE INFO

Article history:

Received 30 July 2021

Revised 19 September 2021

Accepted 11 October 2021

Available online 2 February 2022

Keywords:

Air pollution

PM_{2.5} and O₃ trends

Meteorology

COVID-19 lockdown

ABSTRACT

Recently, air pollution especially fine particulate matters (PM_{2.5}) and ozone (O₃) has become a severe issue in China. In this study, we first characterized the temporal trends of PM_{2.5} and O₃ for Beijing, Guangzhou, Shanghai, and Wuhan respectively during 2018–2020. The annual mean PM_{2.5} has decreased by 7.82%–33.92%, while O₃ concentration showed insignificant variations by -6.77%–4.65% during 2018–2020. The generalized additive models (GAMs) were implemented to quantify the contribution of individual meteorological factors and their gas precursors on PM_{2.5} and O₃. On a short-term perspective, GAMs modeling shows that the daily variability of PM_{2.5} concentration is largely related to the variation of precursor gases ($R = 0.67$ – 0.90), while meteorological conditions mainly affect the daily variability of O₃ concentration ($R = 0.65$ – 0.80) during 2018–2020. The impact of COVID-19 lockdown on PM_{2.5} and O₃ concentrations were also quantified by using GAMs. During the 2020 lockdown, PM_{2.5} decreased significantly for these megacities, yet the ozone concentration showed an increasing trend compared to 2019. The GAMs analysis indicated that the contribution of precursor gases to PM_{2.5} and O₃ changes is 3–8 times higher than that of meteorological factors. In general, GAMs modeling on air quality is helpful to the understanding and control of PM_{2.5} and O₃ pollution in China.

© 2022 The Research Center for Eco-Environmental Sciences, Chinese Academy of Sciences. Published by Elsevier B.V.

* Corresponding authors.

E-mails: zcx2011@ustc.edu.cn (C. Zhang), chliu81@ustc.edu.cn (C. Liu).

Introduction

With the rapid development of industry and urbanization, China's air pollution has become a severe issue during the past decades (Chan et al., 2019; Wang et al., 2017a; Wang et al., 2017b). High concentrations of $PM_{2.5}$ and O_3 may pose a huge threat to public health and are closely related to premature death (Cohen et al., 2017; Zhang et al., 2017). Since 2013, the Chinese government has committed to improving air quality and formulated a series of prevention and control measures, such as the Air Pollution Prevention and Control Action Plan (APPCAP) in 2013 and the Clean Air Action Plan during 2018–2020 (Ding et al., 2019; Ma et al., 2019; Wang et al., 2020b). The annual mean $PM_{2.5}$ concentration dropped by 30% to 50% across China over the 2013–2018 period (Zhai et al., 2019). Although the control of $PM_{2.5}$ has made substantial progress, the slight increase in surface ozone concentration especially for urban areas has brought more complex challenges (Li et al., 2019b; Lu et al., 2018). Compared with 2013, the average 90-th percentiles of maximum daily 8-hour O_3 concentrations increased by 20.1% in 74 cities over China in 2017 (Lu et al., 2020).

Previous studies (e.g., Li et al., 2019b) have proven that strengthening the control of $PM_{2.5}$ precursor emissions may aggravate O_3 pollution due to the complex photochemical interaction between O_3 and $PM_{2.5}$. Strategies that are conducive to reducing $PM_{2.5}$ concentration may change the ratio of NO_x -VOC, thereby adversely affecting the control of O_3 (Lu et al., 2020). In addition, the reduction of $PM_{2.5}$ may inhibit the aerosol absorption of free radicals such as N_2O_5 and HO_2 , which leads to an increase in the oxidation capacity of the atmosphere, and the O_3 concentration is further increased through photochemical reactions (Li et al., 2019a; Lou et al., 2014). However, Tan et al., 2020 argued that HO_2 uptake on aerosol did not significantly affect the ozone production rate in the North China Plain in 2014. It is worth noticing that during the emission control period, meteorological factors (such as temperature, wind, relative humidity, short-wave radiation, etc.) will also have a significant impact on the formation, transportation, and diffusion of $PM_{2.5}$ and O_3 (Cheng et al., 2019; Li et al., 2017). Therefore, in the purpose of realizing the joint control of $PM_{2.5}$ and O_3 , it is necessary to consider the influence of both emissions of precursor gases and meteorological factors.

Due to the COVID-19 epidemic since January 2020, China has adopted a series of shutdown measures, which provided an excellent opportunity to evaluate the response of air pollutants to major emission reductions (Le et al., 2020). The rapid interruption of road traffic and manufacturing has led to a sharp reduction in anthropogenic emissions and a significant improvement in air quality (Wang et al., 2020a). In most cities, the concentration of $PM_{2.5}$ has decreased although the pollution of O_3 has increased slightly (Chu et al., 2021; Sicard et al., 2020). Unexpectedly, cities in northern China, especially Beijing-Tianjin-Hebei (BTH) regions, experienced $PM_{2.5}$ concentration increases during the lockdown (Huang et al., 2020). This unexpected increase is related to the secondary formation of aerosols (Zheng et al., 2020). In addition to strict lockdown measures, the adverse effects of weather conditions are easily overlooked and diffi-

cult to quantify during the COVID-19 lockdown (Wang et al., 2020a).

In this study, an observation-based statistical model, Generalized Additive Model (GAM), is implemented to characterize the nonlinear response of $PM_{2.5}$ and O_3 hourly measurements to meteorological variables and precursor gases for Beijing, Shanghai, Guangzhou, and Wuhan respectively, during 2018–2020. Differ from physical-based models, data-driven statistical techniques including GAMs do not rely on the use of atmospheric principles. Compared to machine learning techniques, GAMs have the advantage of better interpretability, which are rather important for the understanding and control of air pollution. The GAMs model can explicitly quantify the $PM_{2.5}$ and O_3 concentration trends with response to individual covariates including meteorological variables and precursor gases. Based on GAMs analysis, we have quantified the relative contributions of meteorological factors and precursor emissions and assessed the main driving forces for changes in $PM_{2.5}$ and O_3 concentrations before and after the implementation of the lockdown measures for these cities.

This paper is organized as follows: first, we introduced the data and methods that were used; second, we discussed the change trends of $PM_{2.5}$ and O_3 concentrations in the four cities from 2018 to 2020 and the relative contributions of various factors; finally, we described the changes in pollutants during the lockdown.

1. Materials and methods

1.1. Data

Hourly ERA-5 meteorological analyses datasets between 2014–2020 for Beijing, Shanghai, Guangzhou, and Wuhan are available from European Centre for Medium-Range Weather Forecasts (<https://www.ecmwf.int/en/forecasts/datasets/reanalysis-datasets/era5>, last access: 10 Jul 2021). The weather elements include zonal wind (u), meridional wind (v), temperature (T), pressure (P), relative humidity (H), boundary layer height (B), downward shortwave solar radiation (R), and precipitation (I). The hourly pollutant concentration data between 2014–2020 were obtained from the national control site data of the China National Environmental Monitoring Centre (CNEMC). The involved air pollutants include CO, O_3 , $PM_{2.5}$, NO_2 , SO_2 , and PM_{10} . The larger fitted temporal window of data samples more than just the research period of 2018–2020 was used to the GAMs model to avoid model underfitting and improve model robustness.

1.2. Generalized additive model

Generalized additive models were first proposed in 1980s, by generalizing linear regressions and allowing additivity of non-linear variance functions (Hastie and Tibshirani, 1987; Ravindra et al., 2019). GAMs can automatically fit non-linear relationships without having to manually try different transformations (Ravindra et al., 2019).

GAM can use widely distributed (e.g., Normal distributions) response variables, and use logarithm, inverse, and other link functions to measure the influence of explanatory variables

on the response variables. The GAM modeling on the daily pollutant concentration series uses the logarithmic function as the link function, as the following equation:

$$\ln(Y) \sim \alpha + \sum_i^n S(x_i) + \varepsilon \quad (1)$$

where, Y is the hourly series of pollutant concentration; α is the mean value of Y ; $S(x_i)$ is the non-parametric smoothing functions of the i th variates x_i ; and ε is the fitting residual. To ensure the robustness of model fitting, the Restricted Maximum Likelihood (REML) method is selected for smoothness selection.

2. Results and discussion

2.1. Temporal and spatial changes of pollutants

Fig. 1 shows the changes in the annual average concentration of major pollutants in the four cities of Beijing, Shanghai, Wuhan, and Guangzhou from 2018 to 2020. The average relative changes of NO_2 , CO , O_3 , SO_2 , $\text{PM}_{2.5}$ and PM_{10} are -21%, -9.19%, -0.56%, -28.83%, -20.99%, -25.47%, respectively. In most cities, there are significant decreases in NO_2 , SO_2 , $\text{PM}_{2.5}$, and PM_{10} . The annual average mass concentration of $\text{PM}_{2.5}$ dropped from 34.46–47.64 $\mu\text{g}/\text{m}^3$ in 2018 to 22.77–37.82 $\mu\text{g}/\text{m}^3$ in 2020, reflecting the impact of the Clean Air Action Plan control measures and COVID-19 lockdown. The largest reduction in SO_2 is likely to be related to the rapid development of fuel desulphurization technology in industrial production (Jiang et al., 2021; Liu et al., 2018). In contrast, the changes of CO and O_3 showed an increase or decrease with the difference of regions, especially O_3 showed different degrees of increase in Wuhan and Guangzhou, respectively 0.92% and 4.65%. The obvious increase of O_3 is closely related to the decrease of $\text{PM}_{2.5}$. As the decrease of aerosol concentration, higher solar radiation at the ground surface can promote the occurrence of photochemical reactions, which leads to the formation of more ozone (Fan et al., 2020).

Fig. 2 shows the changing trends of NO_2 , CO , O_3 , SO_2 , $\text{PM}_{2.5}$, and PM_{10} on different time scales during the three years from 2018 to 2020 in Beijing. The pollutant concentration changes in the other three cities are shown in the appendix (Figs. S1–S3). Fig. 2 illustrates that each pollutant has an obvious seasonal cycle. Most air pollutants show similar seasonal changes, with high values in winter and low values in summer. Unlike other pollutants, ozone has the opposite seasonality. The high temperature and strong solar radiation in summer make the O_3 concentration significantly higher than that in winter. In addition, the reduction of $\text{PM}_{2.5}$ causes the aerosol deposition rate of HO_2 radicals to slow down, which may also be beneficial to the formation of O_3 (Li et al., 2019a).

In addition to primary emissions including aerosols and their precursor gases, meteorological conditions can also affect the secondary formation and regional transport of aerosols (Chen and Wang, 2015). Many previous studies have shown that in recent years, the significant reduction in pollutant concentration is closely related to the implementation of strict emission control policies, while the effect of meteorological

factors on air quality is relatively small (Liu et al., 2019; Xu et al., 2018). For example, due to the implementation of the Air Pollution Prevention and Control Action Plan (APPCAP), the annual average concentration of $\text{PM}_{2.5}$ in Beijing decreased from 89.5 $\mu\text{g}/\text{m}^3$ in 2013 to 58 $\mu\text{g}/\text{m}^3$ in 2017 (Cheng et al., 2019). In addition, the air quality of cities in China has also undergone significant changes during COVID-19. Determining the relative contribution of favorable weather conditions and emission reduction measures to air quality improvement will help objectively evaluate the effectiveness of air quality control measures. Therefore, this study established a GAM model to quantify the relative contribution of meteorological factors and non-meteorological factors.

2.2. Marginal effect of each covariate

We discussed the marginal effects of various influencing factors on $\text{PM}_{2.5}$ and O_3 based on the data from 2018 to 2020. After considering the selection of the optimal variables, the R^2 of GAM are in a range of 0.68–0.84 for $\text{PM}_{2.5}$ and 0.70–0.82 for O_3 , respectively, indicating that the model can better explain the changes in O_3 and $\text{PM}_{2.5}$ concentrations. To explain the marginal effects of each covariate on the concentration of $\text{PM}_{2.5}$ and O_3 in a more intuitive way, we use $100 \cdot [\exp(S(x_i)) - 1]$ to calculate the relative contribution of the explanatory variable $S(x_i)$ to the response variable in the GAM model (Figs. 3–4 and S4–S9). We choose Beijing as a typical city for analysis. Figs. 3 and 4 discussed various meteorological conditions, i.e., zonal wind (u), meridional wind (v), temperature (T), pressure (P), relative humidity (H), boundary layer height (B), downward shortwave solar radiation (R), and precipitation (J), and the marginal effects of precursor substances such as NO_2 , CO , SO_2 . Note that each marginal effect is denoted by a solid line with a 95% confidence interval (dashed lines), and the vertical lines adjacent to the lower x-axis represent the distributions of these covariates. The EDF for the GAM smooth term is noted inside the bracket of the text. When EDF is not equal to 1, it indicates that there is a nonlinear relationship between the explanatory variable and the response variable, and the larger the value, the more significant the nonlinear relationship (Requia et al., 2019).

During the study period, the EDF of temperature and relative humidity were both greater than 1, indicating a non-linear relationship to the response variable. Dry, hot weather is often associated with high O_3 events. Relative humidity has a certain scavenging effect on O_3 and its precursors, which is significantly negatively correlated with changes in O_3 concentration (Fig. 4e). On the contrary, temperature and O_3 concentration have a significant positive nonlinear relationship. As the temperature increases, the O_3 concentration gradually increases (Fig. 4c). However, a high-humidity and low-temperature environment is conducive to the dissolution of gaseous precursors in liquid aerosols and accelerates the generation of $\text{PM}_{2.5}$ (Chang et al., 2020). Figs. 3c and 3e show that such an effect becomes obvious when the temperature is higher than 275 K and the humidity is higher than 40%.

In addition, Inter-regional pollution transmission is also one of the main reasons for pollutant changes, which is mainly adjusted by wind direction and wind speed. It is well known that wind can dilute the concentration of pollutants

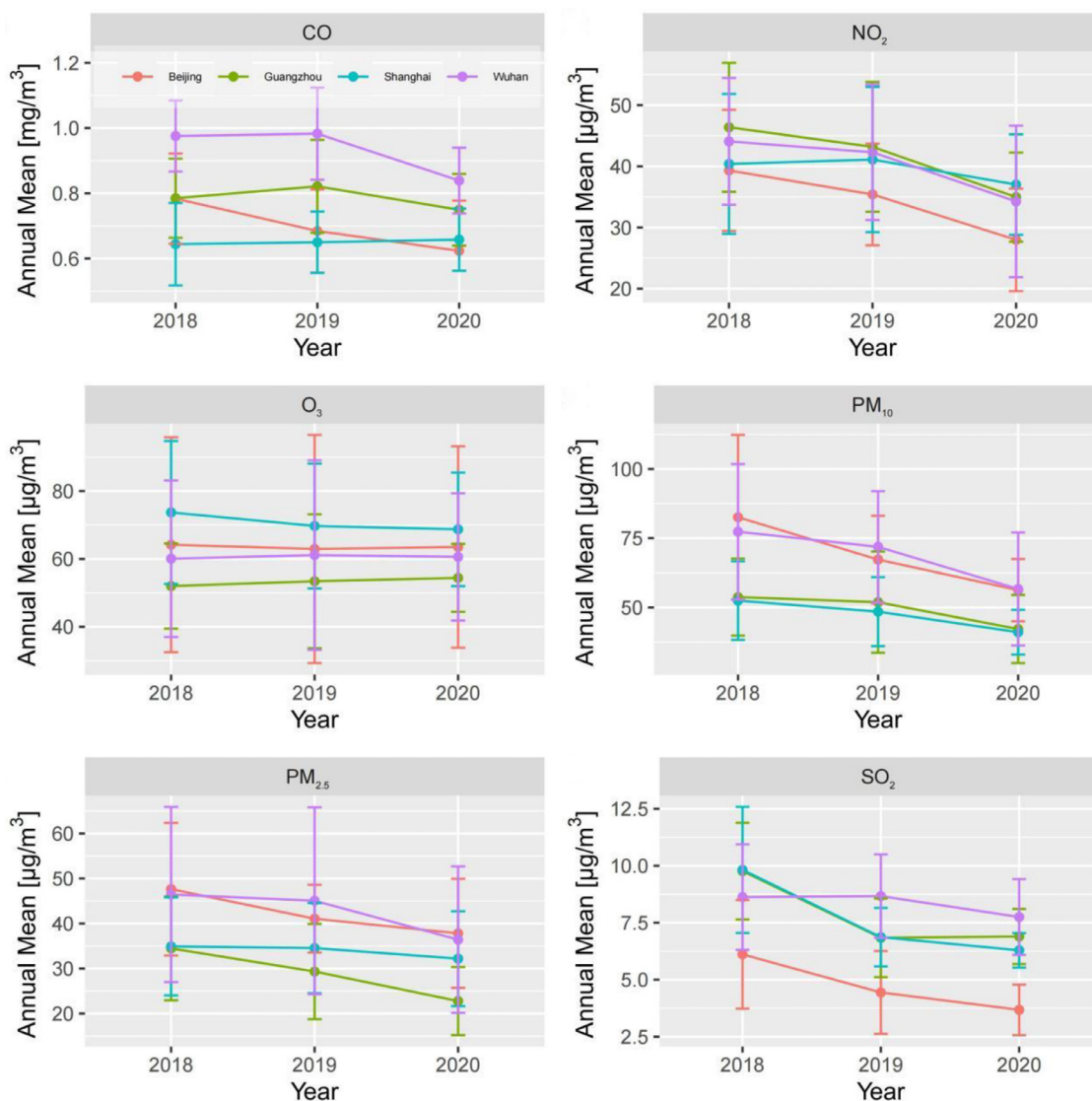


Fig. 1 – The annual mean mass concentrations for six critical air pollutants (SO₂, NO₂, O₃, CO, PM_{2.5}, and PM₁₀) during 2018–2020. The mean values for the six pollutant gases are shown in different colors. Note that error bars are the standard deviations of the monthly average.

and transport precursor substances. However, low wind speed can promote the mixing of pollutants, thereby generating precursor substances such as NO_x, VOCs, and promoting the occurrence of photochemical reactions (Requia et al., 2019). As shown in Fig. 4a–b, when the wind speed is lower than 2m/s, as the wind speed increases, the O₃ concentration increases.

To better understand the relative contribution of non-meteorological factors, we should also focus on the impact of precursor gases on the PM_{2.5} and O₃ variation (Xiang et al., 2020). NO₃⁻ and SO₄²⁻ are generated by the gas-phase reactions of aerosol precursors (NO_x and SO₂), which are important components of secondary aerosols (Liu et al., 2021). Tropospheric O₃ is produced by NO_x and VOCs in sunlight (Wang et al., 2019). When the photo-stationary state between O₃ and NO_x is destroyed by the intervention of RO₂ and HO₂ from VOCs and CO, NO₂ produced by oxidation accumulates O₃ through photolysis (Atkinson, 2000). We can generally see

significant nonlinear relationships between the response variables and various precursor substances. There was an increase in PM_{2.5} concentration when NO₂ and CO increased. Meanwhile, the CI of NO₂ and CO concentration was relatively narrow (Fig. 3i–j). In Fig. 3k, PM_{2.5} decreases with the increase of SO₂, showing a negative correlation, but the CI of SO₂ increases a lot. There was a significantly negative correlation between O₃ concentration and NO₂ (Fig. 4i). (Tobias et al., 2020) pointed out that may be related to the type of O₃ control. Fig. 3l shows that there is a positive correlation between O₃ and PM_{2.5}, which can be understood as a high concentration of ozone that promotes the formation of secondary aerosols (Ding et al., 2013; Zhu et al., 2019).

Additionally, meteorological variables such as boundary layer height, atmospheric pressure, and shortwave radiation also play an important role in the formation, diffusion, and deposition of tropospheric pollutants. In sum, the combined

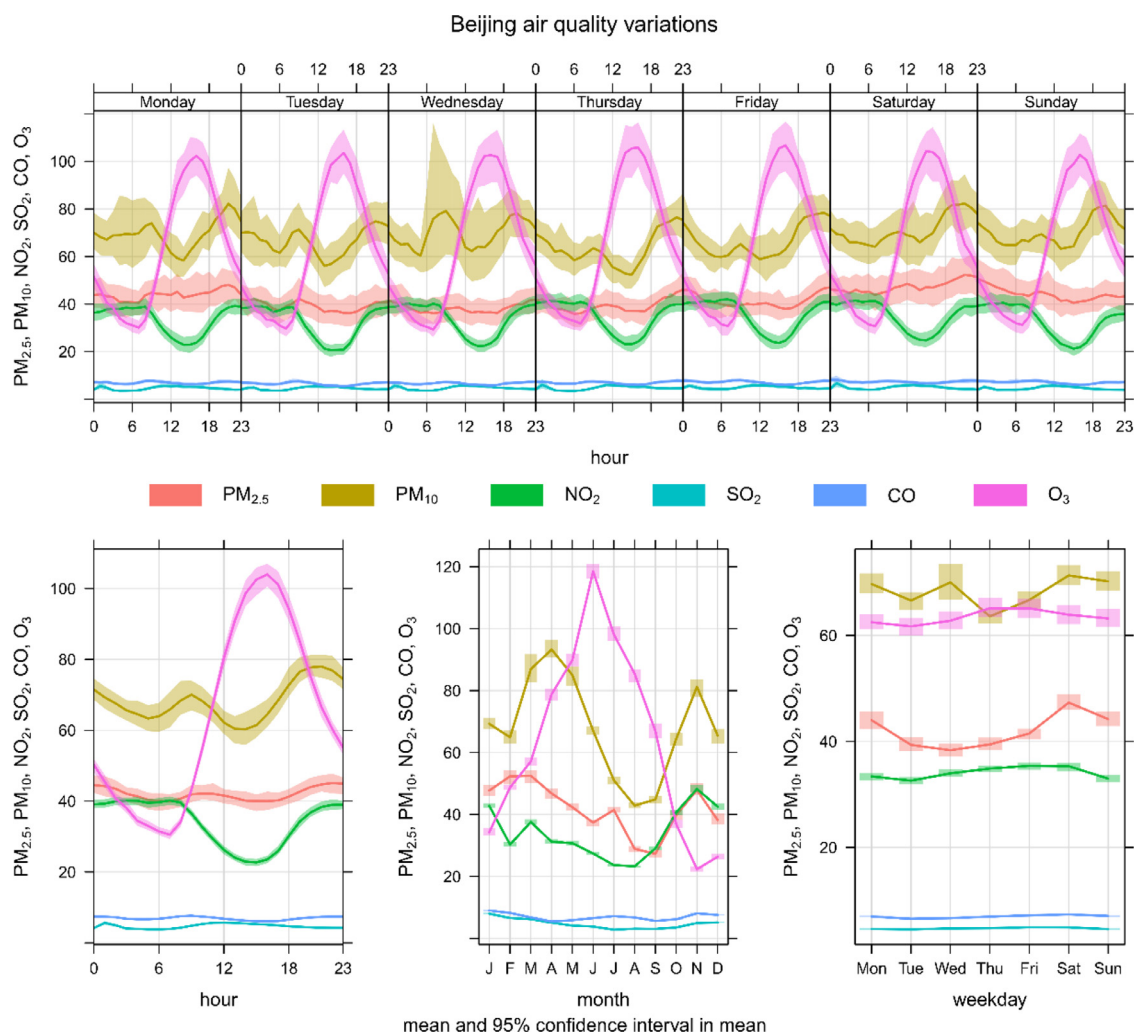


Fig. 2 – The mean concentration of six criteria air pollutants during 2018–2020 on different time scales in Beijing. Note that the mean values of the six pollutant gases are displayed in different colors. Unit: $\mu\text{g}/\text{m}^3$ for SO_2 , NO_2 , O_3 , $\text{PM}_{2.5}$ and PM_{10} ; $100 \mu\text{g}/\text{m}^3$ for CO .

effects of these variables can partially explain the seasonal changes in air pollutants.

Figs. S10 and S11 show the comparison of daily meteorological and non-meteorological smoothing items accumulated during GAM modeling for $\text{PM}_{2.5}$ and O_3 in Beijing, represented by $S(\text{meteos})$ and $S(\text{non_meteos})$ respectively. The gaseous pollutants in several other cities also showed similar results (Figs. S12–S17). For $\text{PM}_{2.5}$, the changing trend of $S(\text{non_meteos})$ in major cities is basically the same as the daily concentration change of $\text{PM}_{2.5}$, and the correlation coefficient (R) is between 0.67–0.90. However, $S(\text{meteos})$ has a poor correlation with daily $\text{PM}_{2.5}$ concentration ($R = 0.17$ –0.59). On the contrary, the daily O_3 concentration changes in major cities are mainly related to the changes in $S(\text{meteos})$ ($R = 0.65$ –0.80) and are less affected by $S(\text{non_meteos})$ ($R = 0.29$ –0.59). Overall, weather and meteorological conditions dominate the daily concentration of O_3 in the troposphere. Especially for megacities, the seasonality in mid-to-high latitude regions is strong, while the daily variation of $\text{PM}_{2.5}$ is dominated by non-meteorological factors.

2.3. Abnormalities during the epidemic

As it could be expected, the implementation of epidemic lockdown measures will cause significant changes in the concentration of pollutants, and also create an opportunity to quantify the impact of artificial control and meteorological conditions on pollutants. Many studies have shown that, during the lockdown period, air pollution levels around the world have dropped significantly (except for ozone) (Kerimray et al., 2020; Nakada and Urban, 2020). It is worth noticing that although $\text{PM}_{2.5}$ concentration in most cities in China has decreased significantly, unexpected increases in $\text{PM}_{2.5}$ concentration have been found in the northern regions (Huang et al., 2020; Wang et al., 2020a).

The concentration differences before and after the lockdown are mainly attributed to the drastic measures to restrict human movement and industrial activities (Otmami et al., 2020). In addition, the role of meteorological factors during the lockdown can not be ignored, but it has not been quantified in most studies (Otmami et al., 2020; Zheng et al., 2020). We

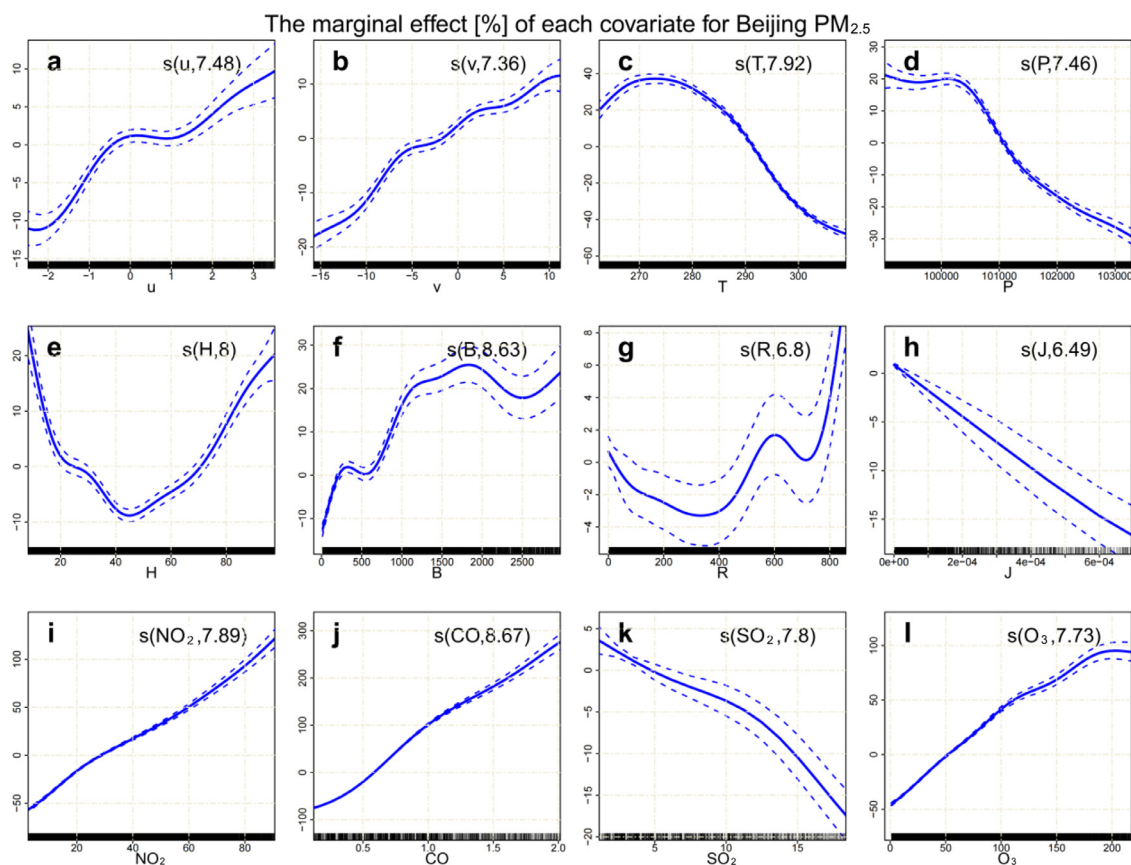


Fig. 3 – Response curves of Beijing's PM_{2.5} concentration to changes in (a) zonal wind, (b) meridional wind, (c) temperature, (d) pressure, (e) relative humidity, (f) boundary layer height, (g) downward shortwave solar radiation, (h) precipitation, (i) NO₂, (j) CO, (k) SO₂ and (l) O₃.

modeled based on the 2014–2020 datasets and discussed the same period from 2019 and 2020 (January 1 to March 12). We used data analysis to study the short-term impact of meteorological factors on urban pollutant concentrations during the epidemic, and the response of air quality to emission control.

We divided January 1 to March 12 into the pre-lockdown period (January 1 to January 24), CNY and COVID-19 period (January 24 to February 19), and post-lockdown period (February 19 to March 12). Figs. 5 and S18–S20 show the changes in pollutant concentrations, meteorological factors, and anthropogenic factors in each city in the three periods of 2019 and 2020, respectively. Compared to the pre-lockdown period, the implementation of the lockdown measures has increased O₃ levels in various cities to varying degrees (4.21 to 33.61 µg/m³), which is considered to be related to less NO_x under the type of VOCs control (Tobias et al., 2020). Due to the significant reduction in vehicle exhaust and industrial production emissions, the PM_{2.5} concentration in Shanghai, Guangzhou, and Wuhan have a significant downward trend (11.05 to 20.87 µg/m³). On the contrary, after the lockdown, Beijing's PM_{2.5} concentration has increased by 36.33 µg/m³.

Our study found that compared to 2019, ozone concentration in each city rose significantly during the 2020 lockdown period, but there were differences between different regions. During the CNY and COVID-19 lockdown, the mass concen-

tration of O₃ in Beijing increased from 30.42 µg/m³ in 2019 to 50.75 µg/m³ in 2020 (Fig. 5a). The increase rates of O₃ in Guangzhou and Wuhan were comparable (38.80% and 48.15%, respectively), which were much higher than the 8.63% and 15.22% in Beijing and Shanghai. The increase in ozone concentration in Shanghai and Wuhan is mainly related to the change of S(non_meteos) (5.56 and 9.29 µg/m³, respectively), which is about three times the contribution of S(meteos). The contributions of the two factors in Beijing and Guangzhou are equal. The difference is that both meteorological factors and human factors in Guangzhou lead to an increase in ozone concentration, while S(meteos) and S(non_meteos) in Beijing have the opposite effect. S(meteos) offset most of the increase in Beijing O₃ (-10.15 µg/m³).

Compared to 2019, the PM_{2.5} mass concentration in Guangzhou, Shanghai, and Wuhan in 2020 has declined by 7.26 to 30.38 µg/m³. S(non_meteos) is the main influencing factor of PM_{2.5} concentration in these cities (4.94–16.34 µg/m³), which is much higher than the contribution of S(meteos) (0.81–3.05 µg/m³). Both S(meteos) and S(non_meteos) are conducive to the reduction of PM_{2.5} concentration in Wuhan, Guangzhou, and Shanghai. The contribution of S(non_meteos) is 5.32–8.27 times that of S(meteos), indicating the reduction of coal combustion in the secondary industry and the cessation of industrial activities were the main reasons for the reduction

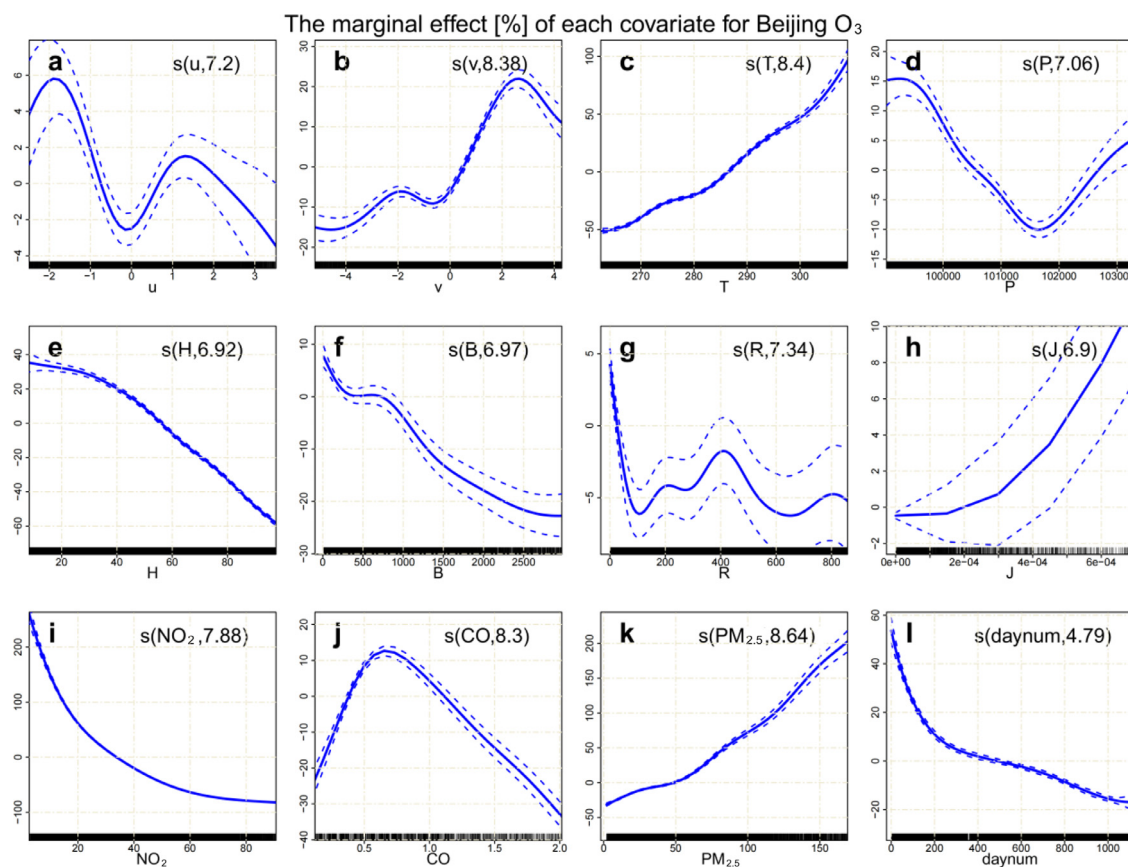


Fig. 4 – Response curves of Beijing’s O₃ concentration to changes in (a) zonal wind, (b) meridional wind, (c) temperature, (d) pressure, (e) relative humidity, (f) boundary layer height, (g) downward shortwave solar radiation, (h) precipitation, (i) NO₂, (j) CO, (k) PM_{2.5} and (l) day number.

of PM_{2.5} concentration during the epidemic. Note that, unlike the above discussion, the mass concentration of Beijing PM_{2.5} increased from 55.99 $\mu\text{g}/\text{m}^3$ in 2019 to 56.88 $\mu\text{g}/\text{m}^3$ in 2020 (Fig. 5b), which is similar to (Huang et al., 2020). Compared to the pre-lockdown period, S(meteos) and S(non_meteos) in Beijing increased by 8.83 and 11.05 $\mu\text{g}/\text{m}^3$ during the CNY and COVID-19 lockdown, respectively, indicating that unfavorable meteorological conditions and strict emission control together led to an abnormal increase in Beijing’s PM_{2.5}.

During the COVID-19 lockdown, Beijing’s frequent temperature inversions, stagnant weather conditions, and high humidity are all conducive to the rapid deposition of atmospheric aerosols (Li et al., 2021). In addition, PM_{2.5} concentration has a complex nonlinear response to non-meteorological factors such as emission control and quadratic forms. Through PM_{2.5} source analysis, Liu et al., 2021 found that SO_4^{2-} of $\text{NO}_3^-/\text{SO}_4^{2-}$ gradually became the dominant component during the Spring Festival. During the lockdown, although mobile emission sources such as transportation were effectively controlled, fixed sources such as household activities and large-scale heavy industries occupied a dominant position, offsetting part of the reduction in PM_{2.5} concentration. Many studies have shown that during the COVID-19, PM_{2.5} tends to decrease in the primary formation and increase in the secondary formation (Huang et al., 2020; Liu et al., 2021; Zheng et al., 2020). Due to the increase of O₃, NO₃ at night

and HO_x free radicals during the day, NOR and SOR are significantly increased, and the atmospheric oxidation capacity is greatly enhanced, which promotes the heterogeneous chemical reaction of SO₂ and NO_x, which is beneficial to the formation of secondary aerosols (Brown et al., 2006; Hallquist et al., 2009; Kroll and Seinfeld, 2008). Therefore, during the COVID-19 outbreak, Beijing’s PM_{2.5} pollution was an abnormal response related to the secondary formation enhancement under adverse weather conditions, still dense stationary source emissions, and enhanced atmospheric oxidation capacity. It is worth noticing that there are differences in PM_{2.5} changes in different regions. The difference in PM_{2.5} trends between Beijing and the other three cities may be related to the net chemical production of inorganic aerosols such as nitrate, sulfate, and ammonium (Huang et al., 2020).

3. Conclusions

In this study, based on the GAMs model analysis, we discussed the temporal trends and influencing factors of PM_{2.5} and O₃ concentrations in Beijing, Guangzhou, Shanghai, and Wuhan, respectively, after the Clean Air Action Plan. Compared to 2018, the PM_{2.5} concentration of the four cities in 2020 all has different degrees of reduction (7.82%–33.92%), while the change of O₃ varies from city to city (–6.77%–4.65%). Our re-

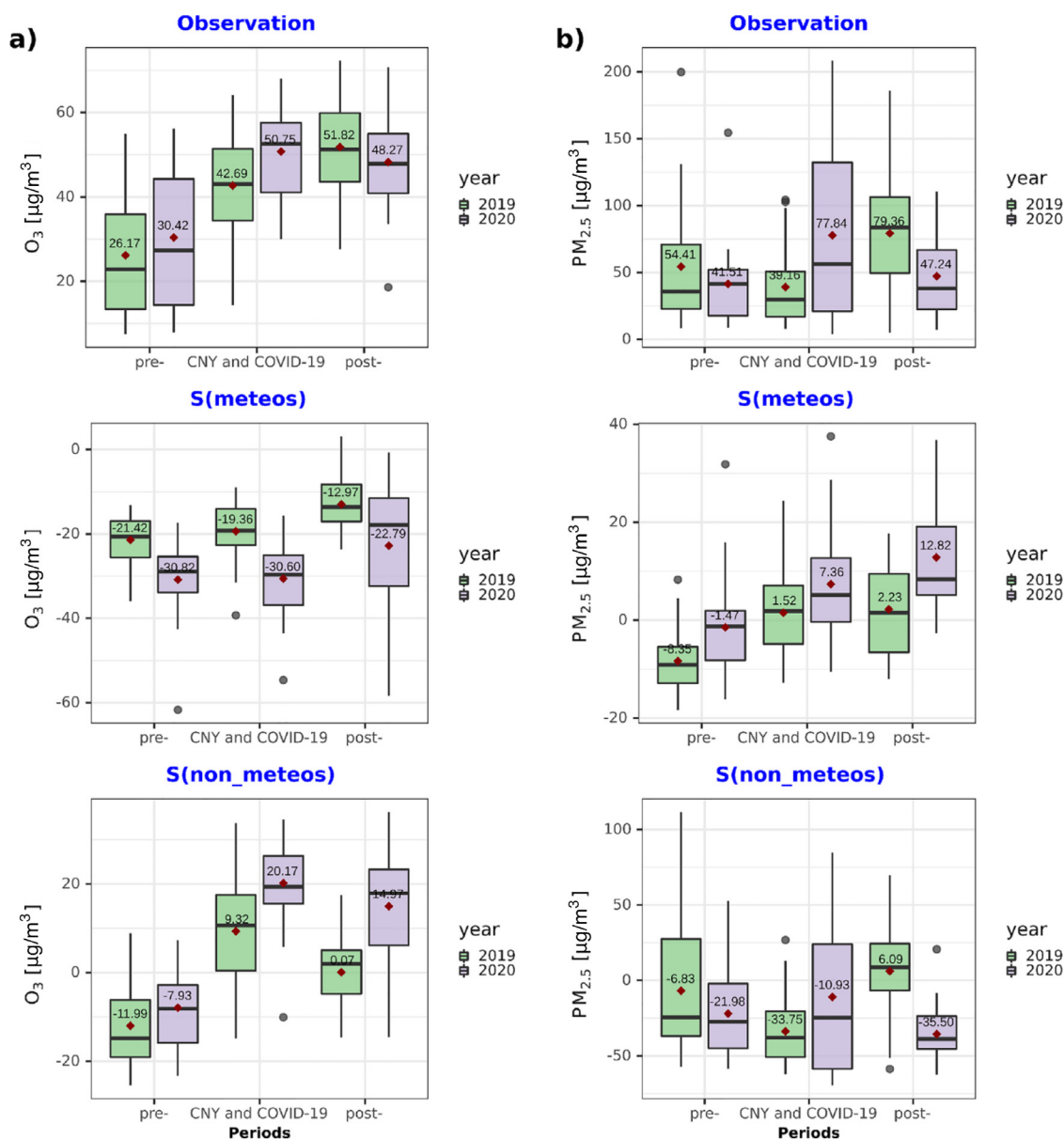


Fig. 5 – The average O₃ (a) and PM_{2.5} (b) measurements and their decomposition by the meteorological and non-meteorological variables in the GAMs modeling. Within each box plot, different years are represented by different colors. The lower and upper bounds of the box plot correspond to the 25th and 75th quartiles, while the solid line represents the median; the top and bottom whiskers extend from the hinges to the largest values by no more than 1.5* IQR (interquartile range) from the hinges. The mean values are noted by red square points with numbers. The black points outside the whisker are outliers.

search results show that after the start of the Clean Air Action Plan, the implementation of the action plan played a leading role in the decrease of daily PM_{2.5} concentration ($R = 0.67-0.90$), and the change of daily O₃ was closely related to meteorological factors ($R = 0.65-0.80$).

This study also investigated the relative contribution of lockdown measures and meteorological factors to changes in PM_{2.5} and O₃ during the COVID-19 lockdown. Unlike previous studies on the air quality changes due to the COVID-19 pandemic (Chan et al., 2021; Song et al., 2021; Zheng et al., 2021), we furtherly decomposed PM_{2.5} and O₃ trends from meteorological

factors by using GAMs modeling. Then, the non-linear relationships between precursor gases and PM_{2.5} or O₃ variations are given in the form of the marginal effect of GAMs, isolated from the impact of meteorology conditions. Compared to chemical model-based analysis (Li et al., 2020; Zheng et al., 2020), our method is rather simple but efficient by only using observational data and statistical models.

Compared to the same period in 2019, the O₃ of the four cities showed varying degrees of growth (8.63%-48.15%) before and after the epidemic. Among them, the changes in O₃ in Guangzhou and Wuhan were more significant (38.80% and

48.15%, respectively), which may be related to strict lockdown measures. In contrast, the PM_{2.5} concentration of Shanghai, Guangzhou, and Wuhan has dropped significantly (14.75%–40.04%), and the relative contribution of human factors is about 5–8 times that of meteorological conditions. However, there has been an unexpected increase in PM_{2.5} concentration in Beijing. The analysis of this study shows that this abnormal situation is caused by the combination of unfavorable weather conditions and the intensive emissions during the CNY and COVID-19 lockdown (8.83 and 11.05 µg/m³, respectively). Therefore, the implementation of GAM to quantify the relative contribution of meteorological conditions and anthropogenic emissions to changes in the concentration of atmospheric pollutants has important guiding significance for the formulation of relevant measures and policies.

Acknowledgments

This research was supported by the National Key Research and Development Program of China (Nos. 2018YFC0213104 and 2017YFC0210002), the National Natural Science Foundation of China (Nos. 41977184, 41941011, and 51778596), the Strategic Priority Research Program of the Chinese Academy of Sciences (No. XDA23020301), the Major Projects of High Resolution Earth Observation Systems of National Science and Technology (No. 05-Y30B01-9001-19/20-3), the Youth Innovation Promotion Association of CAS (No. 2021443), the Young Talent Project of the Center for Excellence in Regional Atmospheric Environment, CAS (CERAE202004), the China Postdoctoral Science Foundation (Nos. 2020TQ0320 and 2021M693068), Anhui Provincial Natural Science Foundation (No. 2108085QD178) and the Fundamental Research Funds for the Central Universities.

Appendix A Supplementary data

Supplementary material associated with this article can be found, in the online version, at [doi:10.1016/j.jes.2021.10.014](https://doi.org/10.1016/j.jes.2021.10.014).

REFERENCES

- Atkinson, R., 2000. Atmospheric chemistry of VOCs and NO(x). *Atmos. Environ.* 34, 2063–2101.
- Brown, S.S., Ryerson, T.B., Wollny, A.G., Brock, C.A., Peltier, R., Sullivan, A.P., et al., 2006. Variability in nocturnal nitrogen oxide processing and its role in regional air quality. *Science* 311, 67–70.
- Chan, K.L., Khorsandi, E., Liu, S., Baier, F., Valks, P., 2021. Estimation of surface NO₂ concentrations over Germany from TROPOMI satellite observations using a machine learning method. *Remote Sens.* 13, 969.
- Chan, K.L., Wang, Z., Ding, A., Heue, K.P., Shen, Y., Wang, J., et al., 2019. MAX-DOAS measurements of tropospheric NO₂ and HCHO in Nanjing and a comparison to ozone monitoring instrument observations. *Atmos. Chem. Phys.* 19, 10051–10071.
- Chang, Y., Huang, R.J., Ge, X., Huang, X., Hu, J., Duan, Y., et al., 2020. Puzzling haze events in china during the coronavirus (COVID-19) shutdown. *Geophys. Res. Lett.* 47, e2020GL088533.
- Chen, H.P., Wang, H.J., 2015. Haze Days in North China and the associated atmospheric circulations based on daily visibility data from 1960 to 2012. *J. Geophys. Res.: Atmos.* 120, 5895–5909.
- Cheng, J., Su, J.P., Cui, T., Li, X., Dong, X., Sun, F., et al., 2019. Dominant role of emission reduction in PM_{2.5} air quality improvement in Beijing during 2013–2017: a model-based decomposition analysis. *Atmos. Chem. Phys.* 19, 6125–6146.
- Chu, B., Zhang, S., Liu, J., Ma, Q., He, H., 2021. Significant concurrent decrease in PM_{2.5} and NO₂ concentrations in China during COVID-19 epidemic. *J. Environ. Sci.* 99, 346–353.
- Cohen, A.J., Brauer, M., Burnett, R., Anderson, H.R., Frostad, J., Estep, K., et al., 2017. Estimates and 25-year trends of the global burden of disease attributable to ambient air pollution: an analysis of data from the Global Burden of Diseases Study 2015. *Lancet* 389, 1907–1918.
- Ding, A.J., Fu, C.B., Yang, X.Q., Sun, J.N., Zheng, L.F., Xie, Y.N., et al., 2013. Ozone and fine particle in the western Yangtze River Delta: an overview of 1 yr data at the SORPES station. *Atmos. Chem. Phys.* 13, 5813–5830.
- Ding, D., Xing, J., Wang, S.X., Liu, K.Y., Hao, J.M., 2019. Estimated contributions of emissions controls, meteorological factors, population growth, and changes in baseline mortality to reductions in ambient PM_{2.5} and PM_{2.5}-related mortality in China, 2013–2017. *Environ. Health Perspect.* 127, 067009.
- Fan, H., Zhao, C.F., Yang, Y.K., 2020. A comprehensive analysis of the spatio-temporal variation of urban air pollution in China during 2014–2018. *Atmos. Environ.* 220, 117066.
- Hallquist, M., Wenger, J.C., Baltensperger, U., Rudich, Y., Simpson, D., Claeys, M., et al., 2009. The formation, properties and impact of secondary organic aerosol: Current and emerging issues. *Atmos. Chem. Phys.* 9, 5155–5236.
- Hastie, T., Tibshirani, R., 1987. Generalized additive models: some applications. *J. Am. Stat. Assoc.* 82, 371–386.
- Huang, X., Ding, A., Gao, J., Zheng, B., Zhou, D., Qi, X., et al., 2020. Enhanced secondary pollution offset reduction of primary emissions during COVID-19 lockdown in China. *Natl. Sci. Rev.* 8, nwaa137.
- Jiang, X., Li, G.L., Fu, W., 2021. Government environmental governance, structural adjustment and air quality: a quasi-natural experiment based on the three-year action plan to win the blue sky defense war. *J. Environ. Manage.* 277, 111470.
- Kerimray, A., Baimatova, N., Ibragimova, O.P., Bukenov, B., Kenessov, B., Plotitsyn, P., et al., 2020. Assessing air quality changes in large cities during COVID-19 lockdowns: the impacts of traffic-free urban conditions in Almaty. *Kazakhstan. Sci. Total Environ.* 730, 139179.
- Kroll, J.H., Seinfeld, J.H., 2008. Chemistry of secondary organic aerosol: formation and evolution of low-volatility organics in the atmosphere. *Atmos. Environ.* 42, 3593–3624.
- Le, T.H., Wang, Y., Liu, L., Yang, J.N., Yung, Y.L., Li, G.H., et al., 2020. Unexpected air pollution with marked emission reductions during the COVID-19 outbreak in China. *Science* 369, 702–706.
- Li, K., Chen, L.H., Ying, F., White, S.J., Jang, C., Wu, X.C., et al., 2017. Meteorological and chemical impacts on ozone formation: a case study in Hangzhou. *China. Atmos. Res.* 196, 40–52.
- Li, K., Jacob, D.J., Liao, H., Shen, L., Zhang, Q., Bates, K.H., 2019a. Anthropogenic drivers of 2013–2017 trends in summer surface ozone in China. *Proc. Natl. Acad. Sci. U. S. A.* 116, 422–427.
- Li, K., Jacob, D.J., Liao, H., Zhu, J., Shah, V., Shen, L., et al., 2019b. A two-pollutant strategy for improving ozone and particulate air quality in China. *Nat. Geosci.* 12, 906–910.
- Li, L., Li, Q., Huang, L., Wang, Q., Zhu, A.S., Xu, J., et al., 2020. Air quality changes during the COVID-19 lockdown over the Yangtze river delta region: an insight into the impact of human activity pattern changes on air pollution variation. *Sci. Total Environ.* 732, 139282.
- Li, M.M., Wang, T.J., Xie, M., Li, S., Zhuang, B.L., Fu, Q.Y., et al., 2021. Drivers for the poor air quality conditions in North China

- plain during the COVID-19 outbreak. *Atmos. Environ.* 246, 118103.
- Liu, L., Zhang, J., Du, R., Teng, X., Hu, R., Yuan, Q., et al., 2021. Chemistry of atmospheric fine particles during the COVID-19 pandemic in a megacity of eastern China. *Geophys. Res. Lett.* 48, 2020GL091611.
- Liu, M.X., Huang, X., Song, Y., Xu, T.T., Wang, S.X., Wu, Z.J., et al., 2018. Rapid SO₂ emission reductions significantly increase tropospheric ammonia concentrations over the North China Plain. *Atmos. Chem. Phys.* 18, 17933–17943.
- Liu, Y., Zheng, M., Yu, M.Y., Cai, X.H., Du, H.Y., Li, J., et al., 2019. High-time-resolution source apportionment of PM_{2.5} in Beijing with multiple models. *Atmos. Chem. Phys.* 19, 6595–6609.
- Lou, S., Liao, H., Zhu, B., 2014. Impacts of aerosols on surface-layer ozone concentrations in China through heterogeneous reactions and changes in photolysis rates. *Atmos. Environ.* 85, 123–138.
- Lu, X., Hong, J., Zhang, L., Cooper, O.R., Schultz, M.G., Xu, X., et al., 2018. Severe surface ozone pollution in China: a global perspective. *Environ. Sci. Technol. Lett.* 5, 487–494.
- Lu, X., Zhang, S., Xing, J., Wang, Y., Chen, W., Ding, D., et al., 2020. Progress of air pollution control in China and its challenges and opportunities in the ecological civilization era. *Engineering* 6, 1423–1431.
- Ma, Z.W., Liu, R.Y., Liu, Y., Bi, J., 2019. Effects of air pollution control policies on PM_{2.5} pollution improvement in China from 2005 to 2017: a satellite-based perspective. *Atmos. Chem. Phys.* 19, 6861–6877.
- Nakada, L.Y.K., Urban, R.C., 2020. COVID-19 pandemic: impacts on the air quality during the partial lockdown in Sao Paulo state, Brazil. *Sci. Total Environ.* 730, 139087.
- Otmami, A., Benchrif, A., Tahri, M., Bounakhla, M., Chakir, E.M., El Bouch, M., et al., 2020. Impact of COVID-19 lockdown on PM₁₀, SO₂ and NO₂ concentrations in Salé City (Morocco). *Sci. Total Environ.* 735, 139541.
- Ravindra, K., Rattan, P., Mor, S., Aggarwal, A.N., 2019. Generalized additive models: Building evidence of air pollution, climate change and human health. *Environ. Int.* 132, 104987.
- Requia, W.J., Jhun, I., Coull, B.A., Koutrakis, P., 2019. Climate impact on ambient PM_{2.5} elemental concentration in the United States: a trend analysis over the last 30 years. *Environ. Int.* 131, 104888.
- Sicard, P., De Marco, A., Agathokleous, E., Feng, Z.Z., Xu, X.B., Paoletti, E., et al., 2020. Amplified ozone pollution in cities during the COVID-19 lockdown. *Sci. Total Environ.* 735, 139542.
- Song, Y., Lin, C., Li, Y., Lau, A.K.H., Fung, J.C.H., Lu, X., et al., 2021. An improved decomposition method to differentiate meteorological and anthropogenic effects on air pollution: a national study in China during the COVID-19 lockdown period. *Atmos. Environ.* 250, 118270.
- Tan, Z., Hofzumahaus, A., Lu, K., Brown, S.S., Holland, F., Huey, L.G., et al., 2020. No evidence for a significant impact of heterogeneous chemistry on radical concentrations in the north China plain in summer 2014. *Environ. Sci. Technol.* 54, 5973–5979.
- Tobias, A., Carnerero, C., Reche, C., Massague, J., Via, M., Minguillon, M.C., et al., 2020. Changes in air quality during the lockdown in Barcelona (Spain) one month into the SARS-CoV-2 epidemic. *Sci. Total Environ.* 726, 138540.
- Wang, Y., Gao, W., Wang, S., Song, T., Gong, Z., Ji, D., et al., 2020b. Contrasting trends of PM_{2.5} and surface-ozone concentrations in China from 2013 to 2017. *Natl. Sci. Rev.* 7, 1331–1339.
- Wang, N., Lyu, X., Deng, X., Huang, X., Jiang, F., Ding, A., 2019. Aggravating O₃ pollution due to NO_x emission control in eastern China. *Sci. Total Environ.* 677, 732–744.
- Wang, S.J., Zhou, C.S., Wang, Z.B., Feng, K.S., Hubacek, K., 2017a. The characteristics and drivers of fine particulate matter (PM_{2.5}) distribution in China. *J. Cleaner Prod.* 142, 1800–1809.
- Wang, T., Xue, L., Brimblecombe, P., Lam, Y.F., Li, L., Zhang, L., 2017b. Ozone pollution in China: A review of concentrations, meteorological influences, chemical precursors, and effects. *Sci. Total Environ.* 575, 1582–1596.
- Wang, P., Chen, K., Zhu, S., Wang, P., Zhang, H., 2020a. Severe air pollution events not avoided by reduced anthropogenic activities during COVID-19 outbreak. *Resour., Conserv. Recycl.* 158, 104814.
- Xiang, S., Liu, J., Tao, W., Yi, K., Xu, J., Hu, X., et al., 2020. Control of both PM_{2.5} and O₃ in Beijing-Tianjin-Hebei and the surrounding areas. *Atmos. Environ.* 224, 117259.
- Xu, Y.L., Xue, W.B., Lei, Y., Zhao, Y., Cheng, S.Y., Ren, Z.H., et al., 2018. Impact of meteorological conditions on PM_{2.5} pollution in China during winter. *Atmosphere* 9, 429.
- Zhai, S.X., Jacob, D.J., Wang, X., Shen, L., Li, K., Zhang, Y.Z., et al., 2019. Fine particulate matter (PM_{2.5}) trends in China, 2013–2018: separating contributions from anthropogenic emissions and meteorology. *Atmos. Chem. Phys.* 19, 11031–11041.
- Zhang, Q., Jiang, X.J., Tong, D., Davis, S.J., Zhao, H.Y., Geng, G.N., et al., 2017. Transboundary health impacts of transported global air pollution and international trade. *Nature* 543, 705–709.
- Zheng, H., Kong, S., Chen, N., Yan, Y., Liu, D., Zhu, B., et al., 2020. Significant changes in the chemical compositions and sources of PM_{2.5} in Wuhan since the city lockdown as COVID-19. *Sci. Total Environ.* 739, 140000.
- Zheng, X., Guo, B., He, J., Chen, S.X., 2021. Effects of corona virus disease-19 control measures on air quality in North China. *Environmetrics* 32, e2673.
- Zhu, J., Chen, L., Liao, H., Dang, R.J., 2019. Correlations between PM_{2.5} and Ozone over China and associated underlying reasons. *Atmosphere* 10, 352.